GROUND-GLASS OPACITY DETECTION BASED ON CORRELATION BETWEEN SUCCESSIVE SLICE IMAGES

HYOUNGSEOP KIM, MASAKI MAEKADO, JOO KOOI TAN, SEIJI ISHIKAWA

Department of Control Engineering, Kyushu Institute of Technology,
1-1, Kitakyushu City, Fukuoka 804-8550, Japan
kim@cntl.kyutech.ac.jp

MASAAKI TSUKUDA

Kyusyu Kouseinenkin Hospital, Japan

Received (Day Month Year)
Accepted (Day Month Year)

Medical imaging systems such as computed tomography, magnetic resonance imaging provided a high resolution image for powerful diagnostic tool in visual inspection fields by physician. Especially MDCT image can be used to obtain detailed images of the pulmonary anatomy, including pulmonary diseases such as the pulmonary nodules, the pulmonary vein, etc. In the medical image processing technique, segmentation is a difficult task because surrounding soft tissues and organs have similar CT values and sometimes contact with each other. We propose a new technique for automatic segmentation of lung regions and its classification for ground-glass opacity from the extracted lung regions by computer based on a set of the thorax CT images. In this paper, we segment the lung region for extraction of the region of interest employing binarization and labeling process from the inputted each slices images. The region having the largest area is regarded as the tentative lung regions. Furthermore, the ground-glass opacity is classified by correlation distribution on the slice to slice from the extracted lung region with respect to the thorax CT images. Experiment is performed employing twenty six thorax CT image sets and 96% of recognition rates were achieved. Obtained results are shown along with a discussion.

Keywords: Ground-glass opacity; Computed tomography; Segmentation; Correlation; Region of interest.

1. Introduction

Medical imaging systems such as computed tomography, magnetic resonance imaging provided a high resolution image for powerful diagnostic tool in visual inspection fields by physician. Especially MDCT image can be used to obtain detailed images of the pulmonary anatomy, including pulmonary diseases such as the pulmonary nodules, the pulmonary vein, etc. Medical imaging systems such as computed tomography, ultrasound imaging or magnetic resonance imaging provided a high resolution images for powerful diagnostic tool in field of computer aided diagnosis system. Image segmentation is one of the important techniques in medical image processing and computer vision. In medical image processing field, some approaches have been reported.

In medical image processing, several approaches have been reported for segmenting of region of interest. N. Ray *et al*. [1] introduced a technique for merging parametric active contours within closed homogeneous image region for MRI segmentation. Furthermore, various imaging techniques are also proposed for detecting abnormal area in the thorax field. In [2], B. van Ginneken *et al.* proposed a technique for lung field segmentation based on image model. For detecting abnormal area, temporal subtraction of lung fields has been performed by K. Doi *et al.* [3-5]. However, manual segmentation of the lung area may require several hours for analysis. Furthermore, Multi-Detector row CT (MDCT) images contain more than 300 slices. Therefore, manual segmentation method cannot apply for clinical application in the MDCT images. Despite various new developments in terms of segmentation of lung region, automatic extraction methods are still very limited.

Ground-Glass Opacity (GGO) [6, 7] is defined as increased attenuation of lung parenchyma without obscuration of the pulmonary vascular markings on CT images. It is one of the important features in lung cancer diagnosis of computer aided diagnosis. It may be seen as diffuse or more often as patchy in distribution taking sometimes a geographic or mosaic distribution. A large number of diseases can be associated with GGO on CT image. If the occupied GGO area is large on the CT image, medical doctor can extract the GGO comparatively easily. However, the possibility to overlook the light gray shadow becomes higher when GGO exists as a small area. Fig. 1 shows an example of GGO shadows with a well-defined margin (shown in cicle). This figure shows 74-year-old male with increased extent of small ground-glass opacity in right upper-lungs zone. Ezoe *et al*. [8] proposed a method for automatic detection of lung cancers using N-Quoit filter. Maekado *et al*. [9] proposed a technique for automatic segmenting the lung regions and extracting the GGO shadows based on gray level histogram. Masutani *et al*. [10, 11] proposed a method for detecting pulmonary embolism in spiral CT angiography based on volumetric image analysis. Brown *et al*. [12] developed a technique for segmenting of the chest CT datasets. It is, however, can be eassily missed by physicians because GGO is measured as faint and tiny shadows on high resolution computed tomography.

In this paper, we propose a method for automatic extracting the lung regions and

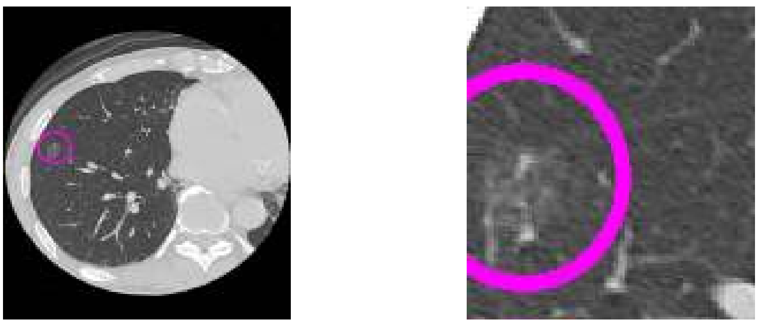

(a) (b)

Fig. 1. An example of CT images of thorax; (a) shows an high resolution through the right upper-lung zone in a 74-year-old male with GGO (circle), (b) shows enlarge of the circle area in (a).

analyzing lung images and specifying ground glass opacity regions. In the first step, region of interests (ROI) is extracted by a pre-processing technique. In the next step, the abnormal area is extracted by comparing the correlation distribution.

This paper is organized as follows. In section 2, we describe an extraction method of lung area and estimation of abnormal area on the candidate area. In section 3, some experimental results are shown. Finally, a discussion and summary are presented in section 4.

2. Methods

2.1. *Segmentation of the lung areas*

This section presents a preprocessing method in proposed segment of the lung regions. We segmented the lung regions to reduce the search space and false positives outside of lung regions. Segmentation of lung regions in our method was separated into two main steps. In the first stage, we segment the thoracic body and lungs employing the pre-processing such as binarization, smoothing and labeling process on given a CT slice image. In the binarization processing, CT values are employed as threshold. Figure 2 shows flow diagrams along with the process of segmentation of the lung areas employing pre-processing technique.

2.2. *Extracting the candidate regions*

In general, lung cancer, GGO shadows or blood vessels come into view as high density. In the second stage, to extract the initial candidates regions, low intensity regions such as background and airway, etc. are removed on the lung regions employing threshold values.

In this stage, we extract the candidate regions of abnormal area such as, GGO shadows on the extracted lung regions. Fig.3 illustrates the flow of the procedure for extracting the initial candidate abnormal area including GGO shadows.

We assume that the *k*-th slice is $S^k(i,j)$ and $S^{k-1}(i,j)$, $S^{k+1}(i,j)$ show prior slice and posterior slice of the *k*-th slice. Correlation coefficient r_{co} is then given by,

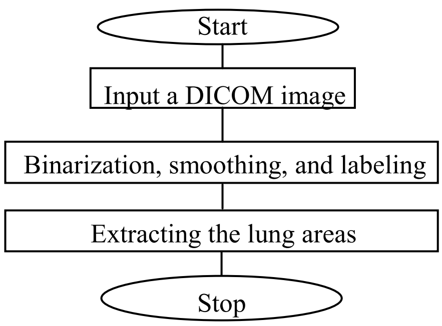

Fig. 2. Flow of the Procedure (Pre-processing).

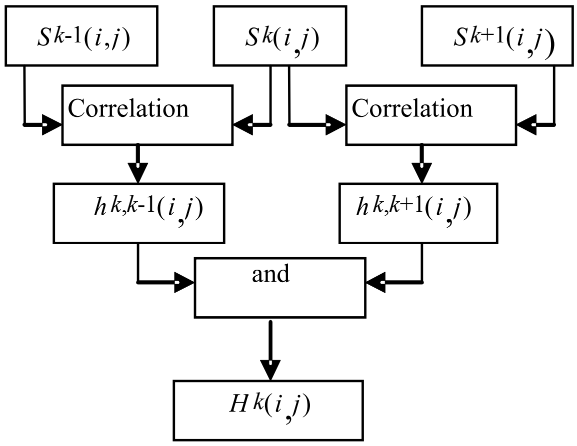

Fig. 3. Flow of the procedure.

$$r_{co} = \frac{\sigma_{fg}}{\sigma_f \sigma_g} \tag{1}$$

where,

$$\sigma_{fg} = \frac{1}{T^2}\int_0^T\int_0^T f(x,y)g(x,y)dxdy\,,$$

$$\sigma_f = \sqrt{\frac{1}{T^2}\int_0^T\int_0^T f^2(x,y)dxdy - \left[\frac{1}{T^2}\int_0^T\int_0^T f(x,y)dxdy\right]^2}$$

$$\sigma_g = \sqrt{\frac{1}{T^2}\int_0^T\int_0^T g^2(x,y)dxdy - \left[\frac{1}{T^2}\int_0^T\int_0^T g(x,y)dxdy\right]^2}\,.$$

T is size of the image $f(x,y)$ and $g(x,y)$. We call created image between successive slice images on the each pair of the [$S^k(i,j)$, $S^{k-1}(i,j)$] and [$S^k(i,j)$, $S^{k+1}(i,j)$], as correlation image. Searching the subset mask size of $m\times m$ pixels, CT values on the mask can be represented in

$$r_1 < r_{co} < r_2 \tag{2}$$

where the threshold parameters m, r_1 and r_2 are decided empirically. That is, correlation images are given by,

$$h_m^{k,k-1}(i_m, j_m) = \begin{cases} S_m^k(i_m, j_m), & if\ r_1 < r_{co} < r_2 \\ CT_{min}^m(i_m, j_m), & else \end{cases} \tag{3}$$

$$h_m^{k,k+1}(i_m, j_m) = \begin{cases} S_m^k(i_m, j_m), & if\ r_1 < r_{co} < r_2 \\ CT_{min}^m(i_m, j_m), & else \end{cases}. \tag{4}$$

Here $CT_{\min}^{m}(i_m, j_m)$ is minimum CT values on the subset mask $m \times m$ pixels of the (i_m, j_m). i_m and j_m are given by,

$$
\begin{aligned}
i_m &= \frac{m-1}{2}, \frac{m-1}{2}+1, \cdots, T-\frac{m-1}{2} \\
j_m &= \frac{m-1}{2}, \frac{m-1}{2}+1, \cdots, T-\frac{m-1}{2}
\end{aligned}.
$$

From the eq.(3) and eq.(4), correlation image $H^k(i,j)$ is represented by logical product of the two images, as

$$
H^k(i,j) = \begin{cases} h^k(i,j), & \text{if } h^{k,k-1}(i,j) > CT_{min} \text{ and } h^{k,k+1}(i,j) > CT_{\min} \\ CT_{min}, & \text{else} \end{cases} \tag{5}
$$

Here CT_{min} is minimum CT value.

2.3. *Classification*

In the final stage, we classify the candidates including ground-glass opacity based on the skewness, entropy and variance.

The skewness is the third momentum and is a parameter showing the extent of how distorted the distribution of a histogram is from symmetric distribution. The skewness S from the normalized histogram $P(i)$ (i=0,1,$\cdots$,n-1) is given by the following equation,

$$
S = \frac{\sum_{i=0}^{n-1} (i-\mu)^3 P(i)}{\sigma^3} \tag{6}
$$

where, μ and σ^2 are mean and variance respectively defined by following equations.

$$
\begin{cases} \mu = \sum_{i=0}^{n-1} iP(i) \\ \sigma^2 = \sum_{i=0}^{n-1} (i-\mu)^2 P(i) \end{cases}
$$

Entropy and variance value are calculated as another feature parameter from the co-occurrence matrix. The co-occurrence matrix is used to estimate the joint probability density function of gray-level pairs in an image in order to obtain the vectors characteristic of the given image. Normalized Entropy E and valiance value V can be computed as,

$$\begin{cases} E = -\sum_{i=0}^{n-1}\sum_{j=0}^{n-1} P_\delta(i,j)\ln\{P_\delta(i,j)\} \\ V = \sum_{i=0}^{n-1}\sum_{j=0}^{n-1}(i-\mu_x)P_\delta(i,j) \end{cases} \tag{7}$$

where,

$$\begin{cases} \mu_x = \sum_{i=0}^{n-1} iP_x(i,j) \\ P_x(i,j) = \sum_{j=0}^{n-1} P_\delta(i,j) \end{cases}$$

and $P_\delta(i,j)$ (i,j=0,1,・・・,n-1) is statistical co-occurrence matrix. In our method, $\delta = (r,\theta)$ of the parameter in $P_\delta(i,j)$ is given as r=1, 10 and θ=4 direction (θ=0, 45, 90, 135). Therefore,

$$P_\delta = \frac{P_{\delta=(r,0^o)} + P_{\delta=(r,45^o)} + P_{\delta=(r,90^o)} + P_{\delta=(r,135^o)}}{4} \tag{8}$$

To classify the unknown data, we plot the three features such as ground-glass opacity, blood vessels of perpendicular and horizontal direction on the 3-D feature space from the extracted known data set for training. In the classification stage, ground-glass opacity, blood vessels of perpendicular direction and horizontal direction are classified onto 3 groups from the extracted three features employing the Mahalanobis distance.

3. Experimental Results

We made an experiment employing 26 cases containing 307 CT slices. Abnormal areas were observed at least one area in all CT data sets. The leave-out method is employed in the classification to exclude biased data sampling. All data sets are separated into three subsets (subset A, subset B and subset C). Three subsets contain normal and abnormal cases. Image of the CT sets were acquired on a Toshiba Medical Systems Scanner. The image size is 512×512 pixels and slices thickness is 2mm. To extract the lung areas, minimum threshold of -1200 H.U. and maximum threshold of -350 H.U. are employed in the prepossessing of the binarization. In the experiment, to extract the candidate abnormal area including GGO shadows, we use the mask size of m 21×21 pixels. The range of the correlation coefficient r_1 and r_2 in eq.(2) r_{co} is 0.5< r_{co} <0.9. Fig. 4 illustrates the experimental results of the pre-processing image.

Table 1 shows the evaluation for proposed system. *TP* is true positive rate, *FN* is false negative rate, *FP* is false positive rate in Table 1, where r=10 in eq. (8). Fig. 5 illustrates the extracted feature such as GGO shadows, blood vessels of perpendicular direction and blood vessels of horizontal direction on the feature space. Fig. 6 shows experimental results of extracting the classified candidate regions.

4. Discussion and Conclusion

To detect the abnormal shadows on MDCT lung images, physician analyzes the segmentation of the lung regions, size of the abnormal area, and texture analysis. Many approaches have been proposed to detect the lung nodules, lung cancer and GGO on the chest radiograph in clinical practice. GGO can be easily missed by physicians because it is measured as faint and tiny shadows on the CT images.

In this paper, we have developed a method for automatic segmentation of lung areas and extraction of ground-glass opacity shadows on the extracted thorax CT images. Fig. 4 (b) shows the segmentation result on selected slice from applying segmentation method based on image preprocessing. In the extracted binarization image, density of lung cancer region or GGO shadows regions are differ to normal area such as blood vessels or airway. In the segment of lung regions, satisfactory experimental results were obtained on all of the thorax CT image sets, automatically.

In order to classify the abnormal area including GGO shadows, we used the skewness, entropy and variance as the statistical feature. Fig. 5 illustrated feature space which extracted 3 patterns, i.e., skewness-entropy, entropy-variance and skewness-variance in experiment. We can observe ground-glass opacity is distributed other tissue such as, the blood vessels in Fig. 5. In Fig. 6, ground glass opacity shadow areas are extracted as

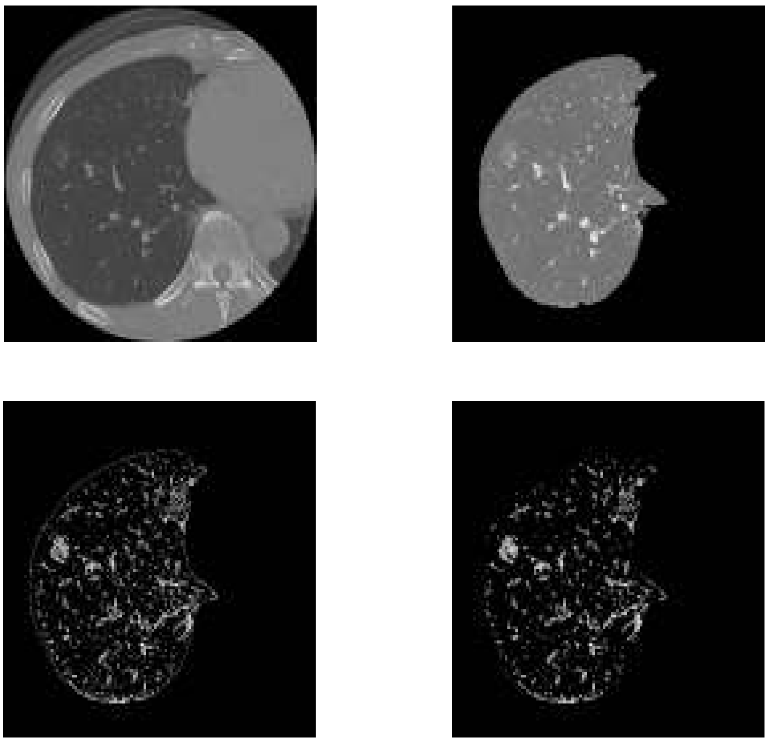

Fig. 4. Experimental results (Pre-processing). (a) shows an original image, (b) shows an extracted lung region, (c) shows an binarized image, (d) shows an smoothing images.

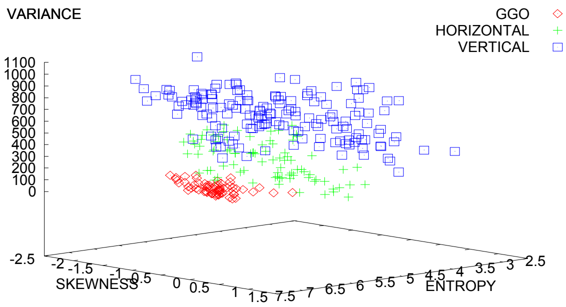

Fig. 5. Feature space.

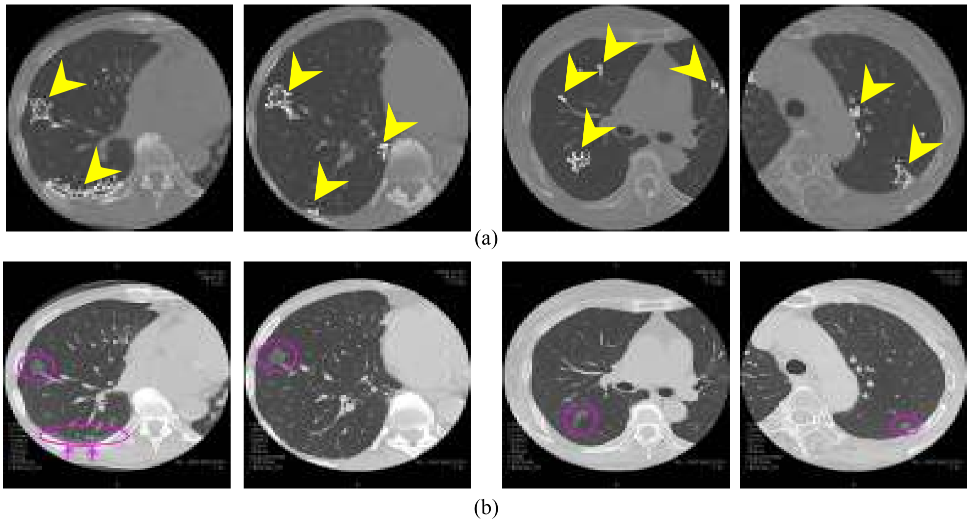

Fig. 6. Experimental results (results the classification of the candidate region). Upper side images are extracted abnormal area by this system (arrow), lower side images show extracted by physician (circle).

arrow regions on the lung CT image correctly. But, some normal areas are misclassified as abnormal area. Fig. 7 shows a misclassified example. It is because the size of ground glass opacity is very small (3mm) and the CT values are almost same between the successive slice images. It is necessary to increase the classification rate. Furthermore, the present experimental system employs Pentium III (CPU; 600MHz, OS; Vine Linux 2.6, Memory; 128MB) PC for image analysis. The processing time of single slice CT image was 30 second in average. We must reduce the execution time for CAD system. It remains as future work.

We made an experiment employing 26 CT cases. From this database, the results were a true positive fraction of 0.7 under the receiver operating characteristic (ROC) analysis. Furthermore, at least one abnormal area is extracted correctly on all CT image sets including abnormal area except only one CT image sets.

In summary, we have presented a method for automatic segmentation of lung areas and ground-glass opacity shadows on the thorax CT image. In order to achieve a higher classification rate, some other statistical features may have been introduced. This remains for further work.

Table 1 Evaluation for proposed system

	Exp. A	Exp. B	Exp. C	Average
TP	71	76	63	70
FN	29	24	37	30
FP	71	68	65	68

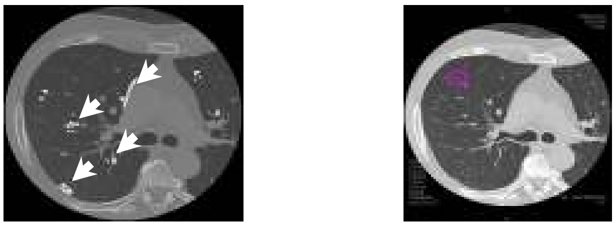

Fig. 7. Experimental results (misclassified). Left hand side images are extracted abnormal area by this system (4 white arrows), right hand side images show extracted by physician (circle).

References

1. N. Ray, S.T. Acton, T.A. Altes *et al.*: "Merging parametric active contours within homogeneous image regions for MRI-based lung segmentation", *IEEE Trans. Med. Imag*, vol. 22, No. 2, 189-199(2003).
2. B. van Ginneken, A. Frangi, J. Staal *et al.*: "Active shape model segmentation with optimal features", *IEEE Trans. Med. Imag*., vol.21, 924-933(2002).
3. A. Kano, K. Doi, H. MacMahon *et al.*: "Digital image subtraction of temporally sequential chest images for detection of interval change", Med. Phys., vol.21, no.3, 453-461(1994).
4. S. Katsuragawa, K. Doi, H. MacMahon: "Image feature analysis and computer-aided diagnosis in digital radiography: Detection and characterization of interstitial lung disease in digital chest radiographs", Med. Phys., vol.15, 311-319(1988).
5. K. Doi, H. MacMahon, S. Katsuragawa *et al.*: "Computer-aided diagnosis in radiology: potential and pitfalls", European Journal of Radiology, vol.31, 97-109(1997).
6. Miller. Jr. WT, Shah RM, "Isolated diffuse ground-glass opacity in thoracic CT: Cause and clinical presentations", AJR, 184, pp.612-622(2005).
7. Austin JH, Muller NL, Freedman PJ, *et al.*, "Glossary of terms for CT of the lungs: recommendations of the nomenclature committee of the fleischner society", Radiology, 200, pp.327-331 (1996).
8. Ezoe T., Takizawa H., Yamamoto S. *et al.*, "Detection method of ground glass opacity from chest x-ray CT images" Progress in Biomedical Optics and Imaging, Vol.3, No. 22, Medical Imaging 2002, Image Processing, Proc. of SPIE, Vol. 4684, pp.1672-1680 (2002).

9. Maekado M., Kim H., Ishikawa S., *et al*., "Automatic extraction of ground-glass opacity on lung CT images by histogram analysis", Intl., Conf., on Control, Automation and Systems, pp.2352-2355(2003).
10. Masutani Y., MacMahon H., Doi K., "Computerized detection of pulmonary embolism in spiral CT angiography based on volumetric image analysis", IEEE Trans. on Medical Imaging, Vol.21, No.12, pp.1517-1523(2002).
11. Masutani Y., MacMahon H., Doi K., "Computer-assisted detection of pulmonary embolism", Proceeding of SPIE (Medical Imaging), pt. II, Vol.3979, pp.944-950(2000).
12. Brown M. S., McNitt-Gray M F., Mankovich N. J., *et al*., "Method fro segmenting chest CT image data using an anatomical model: Preliminary results", IEEE Trans. on Medical Imaging, Vol.16, No.6, pp.828-839(1997).